Journal of Advanced Mechanical Design, Systems, and Manufacturing

Vol. 4, No. 6, 2010

Chatter Stability in Turning and Milling with in Process Identified Process Damping*

Yusuke KURATA**, S. Doruk MERDOL***, Yusuf ALTINTAS***,
Norikazu SUZUKI** and Eiji SHAMOTO**

**Department of Mechanical Engineering, Nagoya University,
Furo-cho, Chikusa-ku, Nagoya, Aichi, 464-8603, Japan
E-mail: kurata@upr.mech.nagoya-u.ac.jp

***Manufacturing Automation Laboratory, University of British Columbia,
2054-6250 Applied Science Lane, Vancouver, BC, V6T 1Z4, Canada

Abstract

Process damping in metal cutting is caused by the contact between the flank face of the cutting tool and the wavy surface finish, which is known to damp chatter vibrations. An analytical model with process damping has already been developed and verified in earlier research, in which the damping coefficient is considered to be proportional to the ratio of vibration and cutting velocities. This paper presents in process identification of the process damping force coefficient derived from cutting tests. Plunge turning is used to create a continuous reduction in cutting speed as the tool reduces the diameter of a cylindrical workpiece. When chatter stops at a critical cutting speed, the process damping coefficient is estimated by inverse solution of the stability law. It is shown that the stability lobes constructed by the identified process damping coefficient agrees with experiments conducted in both turning and milling.

Key words: Chatter, Process Damping, Stability, Plunge Turning, Milling, In Process Identification

1. Introduction

Regenerative chatter vibrations in cutting often result in shortened tool life and a poor surface finish, and therefore must be avoided in practice. The fundamental mechanism of regenerative chatter and its stability have been widely studied and utilized in production [(1),(2)]. The stability laws predict chatter-free depths of cut and speeds as a function of a material's cutting force constant, as well as the relative transfer function between the tool and workpiece structures at the cutting point. The current stability laws can be used only at high speeds where the angular excitation speed, i.e. spindle speed in turning or spindle speed times the number of teeth in milling, is not less than four to five times the dominant natural frequency of the structure. However, many work materials, such as steel and heat-resistant aerospace alloys, cannot be cut at high speeds, but must be machined at speeds lower than the 5^{th}-6^{th} lobes of the system where the current stability laws fail. The contact between the flank face of the tool and the wavy finish surface of the work generated by the vibrations leads to process damping, which suppresses chatter [(3)-(5)]. The contact increases as the cutting speed decreases, hence process damping becomes more dominant at low cutting speeds [(3)].

Researchers have been investigating the modeling of the process damping mechanism, and predicting chatter stability by considering the flank-surface finish contact [(2)]. Hoshi designed an experiment to identify the relationship between cutting velocity and vibration

*Received 9 June, 2010 (No. 10-0245)
[DOI: 10.1299/jamdsm.4.1107]

to support Tobias's argument of cutting force direction variations [4]. Tlusty summarized the research efforts of the CIRP task force, and showed that the clearance angle and tool wear change the dynamic cutting force coefficients significantly [5]. Numerical models have been proposed to predict the process damping force by considering its nonlinearity, such as the amount of contact volume removed and compressed by the flank face of the tool [6]-[8]. However, such nonlinear models are useful mainly for numerical simulation of the process, and cannot readily be used in predicting stability charts. Altintas et al. have proposed a simple linear model, and verified that the damping coefficient is approximately proportional to the ratio of vibration and cutting speeds [9]. They identified the proportionality constant by controlled oscillation tests utilizing a fast tool servo. They predicted stability charts with process damping using Nyquist criterion, and experimentally verified the model. However, their identification method requires a considerable number of tests with a fast tool servo to generate oscillations at the desired frequency, and costly sensors are needed to measure the vibration and the dynamic cutting force.

Suzuki et al. have developed a method to identify the transfer function of a mechanical structure by inverse analysis of the stability limits [10]. The stability is assumed to be free of process damping, and hence this method is applicable only at high speeds, i.e. for the first few lobes of the stability charts. Instead of identifying the structural dynamic parameters of the machine, an inverse solution is used to identify the process damping coefficient in this paper. Structural dynamic parameters are identified off-line through modal tests, and the speed-dependent process damping coefficient is estimated from plunge turning tests. As the tool is fed into the bar center, the cutting speed is reduced continuously, while the feed per revolution and the width of the cut remain constant. Chatter starts initially due to the high cutting speed, but stops at a critical cutting speed as the diameter of the workpiece is reduced. The chatter frequency is measured, and the structural dynamic parameters and cutting conditions are known except for the process damping coefficient. By an inverse solution of the chatter stability expression, the unknown process damping coefficient is estimated and used in constructing stability charts. The estimated process damping coefficient has been tried successfully in predicting stability charts for general turning.

2. Dynamic cutting force model with process damping

The process damping coefficient of a work material is identified from plunge turning tests, and is used in predicting the stability of turning operation in this paper.

2.1 Plunge turning process

A turning tool with a nose radius is used to face-turn a flexible shaft by plunging in the radial direction as shown in Fig. 1. The chip thickness varies along the cutting edge, so as the cutting forces resulting from the nose radius of the tool. For simplicity, the rake face is assumed to be perpendicular to the cutting direction in the current formulation. Although it is inclined in practical turning operations, the inclination is usually small and its effect can be neglected in practice. By adopting Colwell's equivalent chord edge of the tool as shown in Fig. 1, the forces are projected along the chip flow angle η on the xz plane of the rake face and perpendicular to it.

$$F_x = F_c \cos\eta, \quad F_y = -F_t, \quad F_z = F_c \sin\eta \tag{1}$$

Tangential (F_t) and friction (F_c) forces acting on the rake face are modeled as,

$$F_t = K_t h \frac{b}{\cos\eta}, \quad F_c = K_c h \frac{b}{\cos\eta} \tag{2}$$

where b is the width of cut and h is the equivalent chip thickness measured perpendicular to

the chord ($b/\cos\eta$) connecting the two extreme contact points between the tool and the workpiece. Tangential (K_t) and friction (K_c) force coefficients are identified experimentally from vibration-free cutting tests. The chip flow angle ($\eta=\tan^{-1}(F_z/F_x)$) can either be identified from cutting tests, or approximated using the following Colwell's empirical rule when the feed rate c is smaller and the width of cut b is larger than the nose radius R of tools having a zero approach angle [11],

$$\eta = \tan^{-1}\left(\frac{R+\frac{c}{2}}{b-\left(R-\sqrt{R^2-\left(\frac{c}{2}\right)^2}\right)}\right) \tag{3}$$

which has been proven to be sufficiently accurate by the cutting tests conducted in this paper. The source of regenerative chatter is the dynamic fluctuation in the chip flow direction caused by relative vibrations between the tool and the workpiece in the radial and axial directions:

$$h(t) = h_0 - \Delta x(t)\cos\eta - \Delta z(t)\sin\eta \tag{4}$$

where h_0 is the static equivalent chip thickness and regenerative vibrations are

$$\left.\begin{aligned}\Delta x(t) &= x(t) - x(t-T)\\ \Delta z(t) &= z(t) - z(t-T)\end{aligned}\right\}. \tag{5}$$

The time delay T is the spindle rotation period in a turning operation. The vibrations are predicted from the experimentally identified transfer functions as:

$$\begin{aligned}x(s) &= \Phi_{xx}(s)F_x(s) + \Phi_{xy}(s)F_y(s)\\ z(s) &= \Phi_{zz}(s)F_z(s) + \Phi_{zy}(s)F_y(s)\end{aligned} \tag{6}$$

where $\Phi_{xx}(s)$, $\Phi_{xy}(s)$ are the direct and cross transfer functions in the radial direction, and $\Phi_{zz}(s)$, $\Phi_{zy}(s)$ are the direct and cross transfer functions in the axial direction. Depending on the tool geometry and mode shapes of the structure, more transfer functions may need to be considered if they affect regenerative chip thickness. The flexibilities of both the tool and workpiece are considered by simply adding their transfer functions arithmetically. The dynamic cutting force in the direction of chip flow or equivalent chip thickness is expressed as [9]:

$$F_c(t) = \frac{b}{\cos\eta}\left\{K_c\left[h_0 - \Delta x(t)\cos\eta - \Delta z(t)\sin\eta\right] - \underbrace{\frac{C_d}{V}\left[\dot{x}(t)\cos\eta + \dot{z}(t)\sin\eta\right]}_{F_d}\right\}. \tag{7}$$

where the added term F_d is the process damping force, which is proportional to process damping coefficient C_d and the ratio of vibration velocity ($\dot{x}(t)\cos\eta + \dot{z}(t)\sin\eta$) over cutting speed ($V=\pi D/T$, D: diameter of workpiece). The static equivalent chip thickness h_0 is dropped for the stability analysis, and the dynamic cutting force (Eq. (7)) is transformed into Laplace domain as:

$$F_c(s) = -\frac{b}{\cos\eta}\left\{\left[K_c(1-e^{-sT}) + s\frac{C_d}{V}\right]\left[\Phi_{xx}(s)F_x(s)\cos\eta + \Phi_{zz}(s)F_z(s)\sin\eta\right]\right.$$
$$\left. + \left[K_t(1-e^{-sT}) + s\frac{C_d}{V}\right]\left[\Phi_{xy}(s)\cos\eta + \Phi_{zy}(s)\sin\eta\right]F_y(s)\right\}$$
$$F_c(s) = -b\left\{\left[K_c(1-e^{-sT}) + s\frac{C_d}{V}\right]\left[\Phi_{xx}(s)\cos\eta + \Phi_{zz}(s)\frac{\sin^2\eta}{\cos\eta}\right]\right.$$
$$\left. - \left[K_t(1-e^{-sT}) + s\frac{C_d}{V}\right]\left[\Phi_{xy}(s) + \Phi_{zy}(s)\frac{\sin\eta}{\cos\eta}\right]\right\}F_c(s). \quad (8)$$

The critical stability limit is evaluated in the frequency domain by substituting $s=i\omega$ and considering the real and imaginary parts of the frequency response functions (FRFs, $\Phi(i\omega)=G(\omega)+iH(\omega)$). The resulting characteristic equation of the dynamic cutting force in the direction of equivalent chip thickness becomes:

$$\left[1 + b_{\lim}\left(\alpha_1 G_{direct} - \beta H_{direct} - \alpha_2 G_{cross} + \beta H_{cross}\right)\right]$$
$$+i\left[b_{\lim}\left(\alpha_1 H_{direct} + \beta G_{direct} - \alpha_2 H_{cross} - \beta G_{cross}\right)\right] = 0 \quad (9)$$

where

$$\alpha_1 = K_c(1-\cos\omega_c T), \quad \alpha_2 = K_t(1-\cos\omega_c T), \quad \beta = \sin\omega_c T + \omega_c\frac{C_d}{V}$$
$$G_{direct} = G_{xx}\cos\eta + G_{zz}\frac{\sin^2\eta}{\cos\eta}, \quad H_{direct} = H_{xx}\cos\eta + H_{zz}\frac{\sin^2\eta}{\cos\eta}$$
$$G_{cross} = G_{xy} + G_{zy}\frac{\sin\eta}{\cos\eta}, \quad H_{cross} = H_{xy} + H_{zy}\frac{\sin\eta}{\cos\eta}, \quad V = \frac{\pi D}{T}.$$

The characteristic equation can be used for the prediction of chatter stability if the process damping coefficient is known. As the coefficients are the functions of spindle period T, chatter frequency ω_c and chip flow angle η, the width of cut b is searched iteratively using Nyquist stability criterion. The iteration starts by selecting a spindle period T, and the width of cut b is scanned from zero to higher values in fine increments. The chip flow angle η for the trial width of cut b is calculated. The trial chatter frequency ω_c is substituted into the real part of the characteristic equation to find the critical width of cut.

$$b_{\lim} = \frac{-1}{\alpha_1 G - \beta H - \alpha_2 G_{xy} + \beta H_{xy}} \quad (10)$$

The characteristic equation is updated with the new chip flow angle η corresponding to estimated b_{lim}, and the iteration is continued until the critical width of cut converges to a constant value. The chatter frequency ω_c is scanned around natural modes to find the stability limit where the imaginary part becomes zero.

$$\alpha_1 H + \beta G - \alpha_2 H_{xy} - \beta G_{xy} = 0 \quad (11)$$

The process is repeated for each spindle speed to construct the stability chart. The analysis is illustrated in the flow chart shown in Fig. 2.

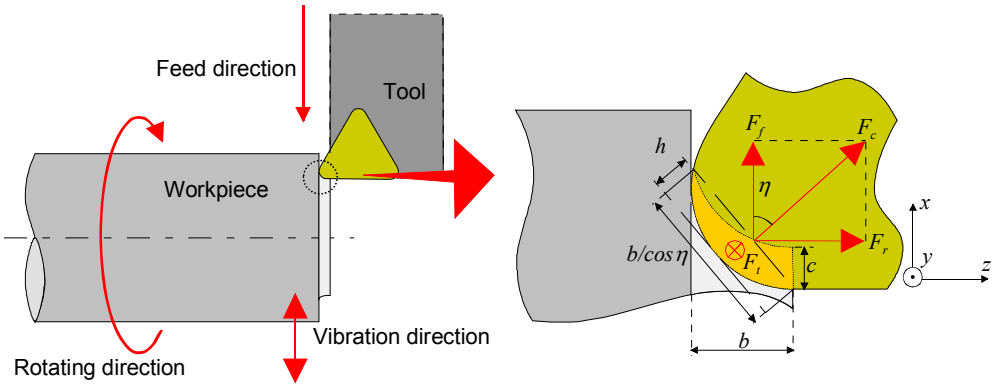

Figure 1 Schematic illustration of plunge turning process

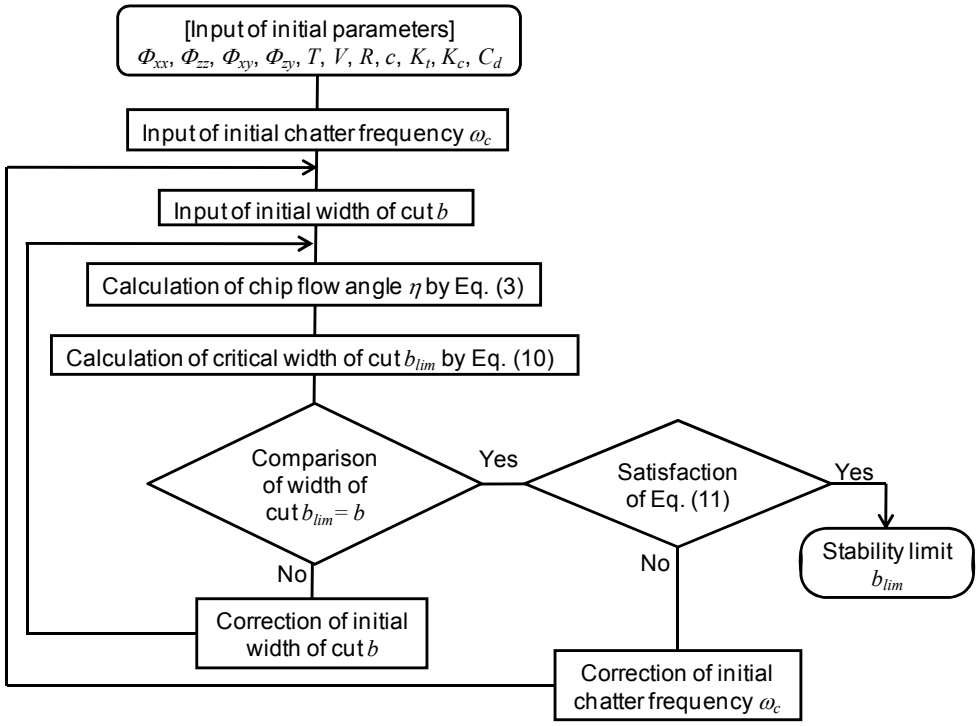

Figure 2 Flow chart of analytical model

2.2 Identification of Process Damping Coefficient

It is known that the critical width of a cut increases as the cutting speed decreases in machining, which is attributed to process damping or the contact between the flank face of the tool and the vibration marks left on the finished surface [9]. Therefore, the process damping coefficient C_d can be identified from cutting tests using the stability equation expressed in Eq. (9). In order to identify it, a cutting test was conducted with a flexible workpiece. The experimental setup used in the plunge turning process is shown in Fig. 3. First, in order to identify the cutting coefficients, a short, rigid shaft of AISI 1045 steel with a hardness of 21 HRc, a length of 70 mm and a diameter of 38.1 mm is face-turned with a TNMA160408 cutting tool having a 0.8 mm nose radius. The tool and workpiece geometry are given in Table 1 and the cutting conditions are given in Table 2. The cutting forces were measured in three directions F_x, F_y, F_z. The chip flow angle, predicted from experimental measurements (η=tan^{-1}(F_z/F_x)), showed good agreement with the Colwell's geometric model given in Eq. (3). The cutting force coefficients were identified from tangential and friction forces as K_t = 2240 MPa and K_c =1580 MPa.

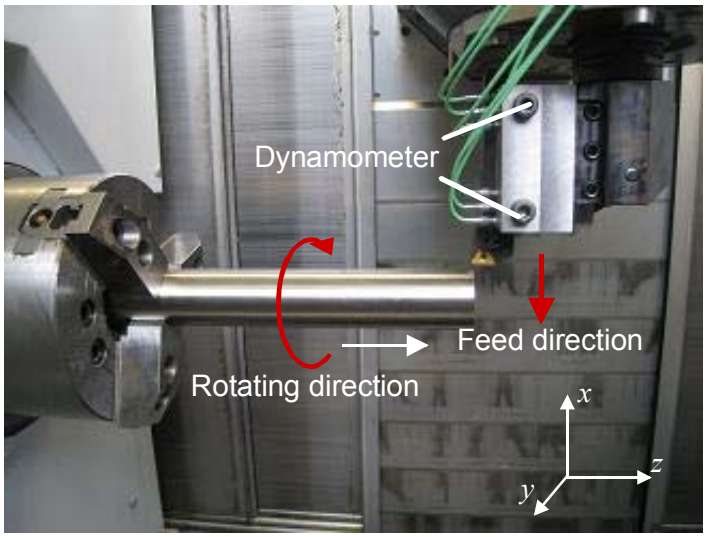

Figure 3 Experimental setup

Table 1 Tool and workpiece geometry

Insert	Type	TNMA160408
	Nose radius R mm	0.8
Workpiece	Material	AISI 1045
	Diameter D mm	38.1

Table 2 Cutting conditions used in cutting coefficient identification

Feed rate c mm/rev	0.06, 0.08, 0.10, 0.12, 0.14
Width of cut b mm	1.0
Spindle speed n min^{-1}	2000

The shaft length was set to 200 mm and the FRFs were measured at its free end with impulse modal tests. The direct and cross FRFs Φ_{xx}, Φ_{xy} had a dominant mode at ω_n =289 Hz with stiffness and damping ratios of k_{xx} =8.9 N/μm, ζ_{xx} =0.012 and k_{xy} =72 N/μm, ζ_{xy} =0.009, respectively. The tool had a natural frequency of 900 Hz with a dynamic stiffness 50 times higher than that of the workpiece, hence it was considered to be rigid.

The cutting forces and sound were measured as the tool was fed into the free end of the shaft in the radial direction. The results are shown in Fig. 4. The spindle speed and width of cut were kept constant at n=1000 min^{-1} and b=0.7 mm during the test. As the diameter of the shaft was reduced continuously from 38.1 mm to zero, the corresponding cutting speed also varied from 119.6 m/min to zero. The cutting force measurements indicate that the process chattered until Zone 2, where chatter diminished as a result of process damping at 4.8 s corresponding to a shaft diameter of 22 mm and a cutting speed of 69.1 m/min.

The process damping coefficient C_d is evaluated from both real and imaginary parts of the characteristic Eq. (9) by scanning the chatter frequency ω_c around the natural modes of the structure. From Eq. (10), C_d is expressed as follows, which is the condition in which the real part of Eq. (9) becomes zero:

$$C_d = -\frac{V_{\lim}}{\omega_c}\left(\frac{\frac{1}{b}+\alpha_1 G_{direct}-\alpha_2 G_{cross}}{H_{direct}-H_{cross}}-\sin\omega_c T\right). \tag{12}$$

From Eq. (11), C_d is expressed as follows, which is the condition in which the imaginary part of Eq. (9) becomes zero:

$$C_d = -\frac{V_{\lim}}{\omega_c}\left(\sin\omega_c T + \frac{\alpha_1 H_{direct} - \alpha_2 H_{cross}}{G_{direct} - G_{cross}}\right). \tag{13}$$

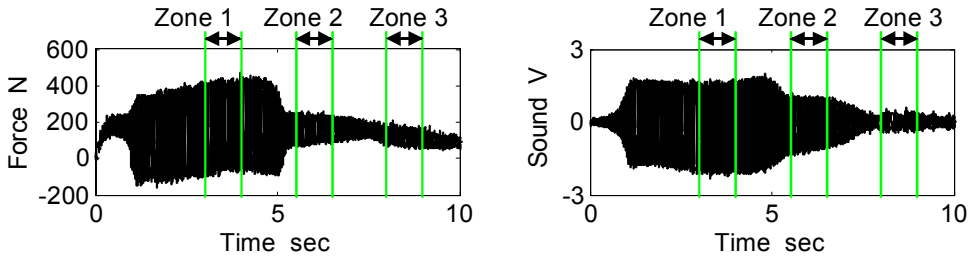

(a) Cutting force and sound measurement

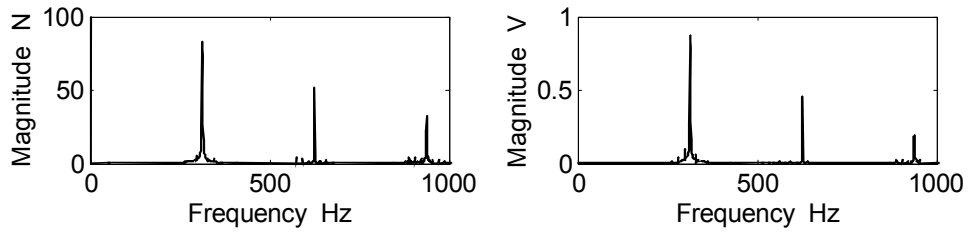

(b) Frequency spectrum of measurements in Zone 1

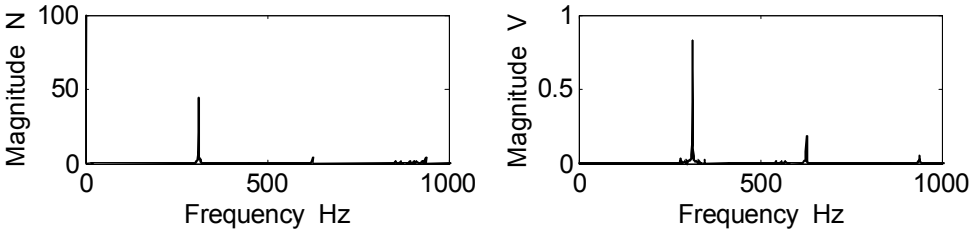

(c) Frequency spectrum of measurements in Zone 2

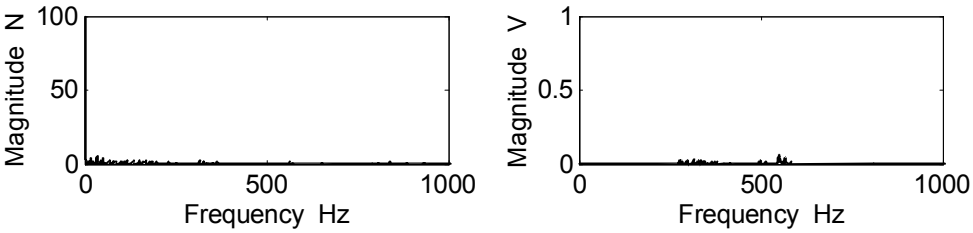

(d) Frequency spectrum of measurements in Zone 3

Figure 4 Vibration measured during cutting

As shown in Fig. 5, if the evaluated process damping coefficients C_d from both the real and imaginary parts of the characteristic equation converges to each other, the solution is accepted. Otherwise, the iteration continues with a new chatter frequency.

Further plunge turning process tests were conducted to investigate the effect of flank wear on the process damping coefficient. Flank wear was measured as soon as the chatter diminished during plunge turning process. Table 3 shows the relation of flank wear VB, critical cutting speed V_{lim} and identified process damping coefficient C_d. Process damping and the corresponding cutting speed increased by about 12 % when flank wear was doubled from 0.15 mm to 0.31 mm. It is evident that once the rubbing between the flank and wavy surface finish reach a critical level, process damping does not increase significantly along with accelerated flank wear.

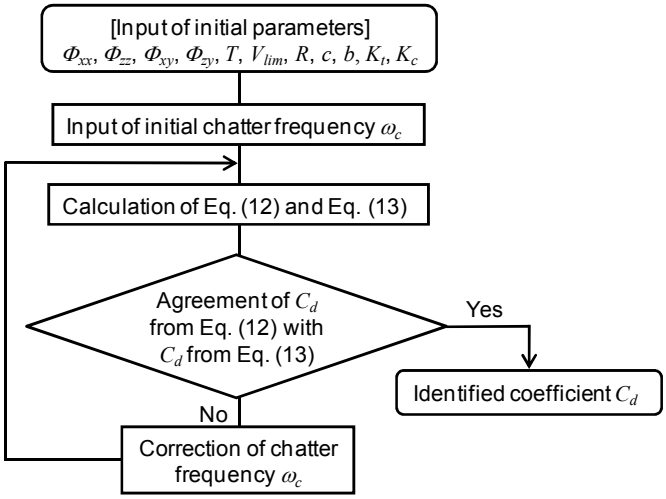

Figure 5 Flow chart of identification of process damping coefficient

Table 3 Effect of flank wear on process damping

Flank wear VB mm	Cutting speed V_{lim} m/min	Process damping coefficient C_d N/μm
0.15	63.8	0.37
0.24	66.0	0.39
0.27	69.1	0.42
0.31	72.3	0.43

3. Chatter Stability of Milling with Process Damping

The dynamic milling forces are modeled in a similar method as presented by Altintas and Budak [12], but including process damping components. Tangential (F_{tj}) and radial (F_{rj}) cutting forces acting on the flute (j) are expressed from Fig. 6 as follows:

$$\begin{cases} F_{tj} = aK_t\left[\Delta x \sin\left(\phi_j\right) + \Delta y \cos\left(\phi_j\right)\right] g\left(\phi_j\right) \\ F_{rj} = a\left[\left(K_r \Delta x + \frac{C_i}{V}\dot{x}\right)\sin\left(\phi_j\right) + \left(K_r \Delta y + \frac{C_d}{V}\dot{y}\right)\cos\left(\phi_j\right)\right] g\left(\phi_j\right) \end{cases} \tag{14}$$

where ϕ_j is the immersion angle of the flute, a is the axial depth of cut, and $g(\phi_j)$=1 when the tooth is in the cut, and zero otherwise. K_t and K_r are static cutting force coefficients in tangential and radial directions. The cutting forces are projected into feed (x) and normal (y) directions, and the contributions of all teeth are summed.

$$F_x = \sum_{j=0}^{N-1}\left[-F_{tj}\cos\left(\phi_j\right) - F_{rj}\sin\left(\phi_j\right)\right], \quad F_y = \sum_{j=0}^{N-1}\left[F_{tj}\sin\left(\phi_j\right) - F_{rj}\cos\left(\phi_j\right)\right] \tag{15}$$

where F_x and F_y are the cutting forces in the x and y directions. Similarly to the turning process and as presented by Altintas et al. [9], the dynamic cutting force vector $\{F_x\ F_y\}^T$ can be expressed as follows:

$$\begin{Bmatrix} F_x \\ F_y \end{Bmatrix} = \frac{a_{\lim}}{2}\left[K_t\left(1 - e^{-i\omega T}\right)\left[A_0{}^t\right] + \left[K_r\left(1 - e^{-i\omega T}\right) + i\frac{C_d}{V}\right]\left[A_0{}^r\right]\right][\Phi]\begin{Bmatrix} F_x \\ F_y \end{Bmatrix} \tag{16}$$

where T is the tooth passing period, a_{lim} is the critical axial depth of cut. The relative frequency response function matrix [Φ] between the tool and the workpiece is obtained by

impulse tests. $[A_0{}^t]$ and $[A_0{}^r]$ are the average directional coefficient matrixes in tangential and radial directions, respectively.

$$\left[A_0{}^t\right]=\begin{bmatrix}\frac{N}{4\pi}\left[\cos(2\phi)\right]_{\phi_{st}}^{\phi_{ex}} & \frac{N}{4\pi}\left[-\sin(2\phi)-2\phi\right]_{\phi_{st}}^{\phi_{ex}}\\ \frac{N}{4\pi}\left[-\sin(2\phi)+2\phi\right]_{\phi_{st}}^{\phi_{ex}} & \frac{N}{4\pi}\left[-\cos(2\phi)\right]_{\phi_{st}}^{\phi_{ex}}\end{bmatrix}$$
$$\left[A_0{}^r\right]=\begin{bmatrix}\frac{N}{4\pi}\left[\sin(2\phi)-2\phi\right]_{\phi_{st}}^{\phi_{ex}} & \frac{N}{4\pi}\left[\cos(2\phi)\right]_{\phi_{st}}^{\phi_{ex}}\\ \frac{N}{4\pi}\left[\cos(2\phi)\right]_{\phi_{st}}^{\phi_{ex}} & \frac{N}{4\pi}\left[-\sin(2\phi)-2\phi\right]_{\phi_{st}}^{\phi_{ex}}\end{bmatrix} \quad (17)$$

where ϕ_{st} and ϕ_{ex} are the entry and exist angles of the cutter. The characteristic equation of the milling system with process damping is constructed from Eq. (16):

$$\det\left\|[I]-\frac{a_{\lim}}{2}\begin{bmatrix}K_t\left(1-e^{-i\omega T}\right)\left[A_0{}^t\right]+\\ \left[K_r\left(1-e^{-i\omega T}\right)+i\frac{C_j}{V}\right]\left[A_0{}^r\right]\end{bmatrix}[\Phi]\right\|=0 \quad (18)$$

where $[I]$ is an identity matrix.

The process damping coefficient (C_d) is assumed to be the same as identified from plunge turning tests. The critical stable axial depth of cut can be evaluated iteratively in a similar fashion with a plunge turning case using Nyquist stability criteria.

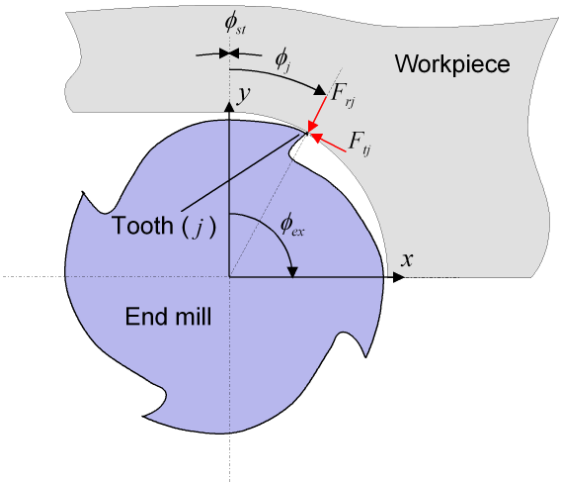

Figure 6 Milling process model

4. Chatter Stability Tests

The predicted chatter stability charts with process damping coefficients were experimentally validated for both plunge turning process and milling as follows.

4.1 Plunge turning Tests

A series of plunge turning tests were conducted using the same experimental setup used in the process damping identification experiments as shown in Table 4. An average process damping coefficient of C_d=0.4 N/μm was used in the predicted chatter stability charts shown in Fig. 7. The predicted stability chart agreed with the chatter experiments when process damping is included. However, the stable widths of cuts are severely underpredicted when the damping is neglected, especially at speeds below 1500 min^{-1}.

Table 4 Cutting conditions to verify analytical model

Feed rate c mm/rev	0.10
Width of cut b mm	0.5-1.3
Spindle speed n min^{-1}	400-2180

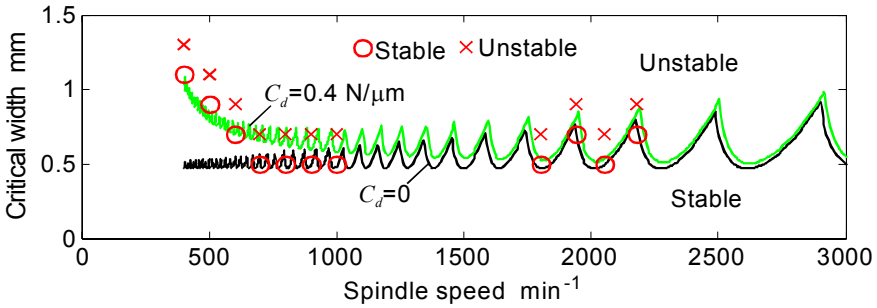

Figure 7 Experimental results and predicted stability charts

4.2 Milling Tests

A series of milling tests on AISI 1045 steel were conducted. A cutter with two inserts was used, and the cutting forces and sound data were recorded during milling tests as shown in Fig. 8. The cutting force coefficients were identified mechanistically from vibration-free milling tests as K_t =1953 MPa and K_r =1186 MPa. The process damping coefficient was assumed to be the same as that identified from the plunge turning process tests (C_d=0.4 N/μm), although the inserts were different. A workpiece clamped to a dynamometer was measured and found to be significantly more rigid than the cutter. The modal parameters of the cutter, cutting tool geometry and cutting conditions are given in Table 5. A chatter stability chart was predicted with and without process damping as shown in Fig. 9. The chatter tests were conducted at 0.05 mm depth increments until chatter occurred. The process damping effect is clearly noticed at speeds below 2000 min^{-1}. Discrepancies between the analytical and predicted stability limits at low speeds are attributed to the use of different inserts than in plunge turning where the process damping coefficient was identified, as well as the neglected effect of changing tool wear. Furthermore, the time variation of directional factors was neglected by averaging them over a tooth period. Nevertheless, the prediction accuracy is acceptable for use in production.

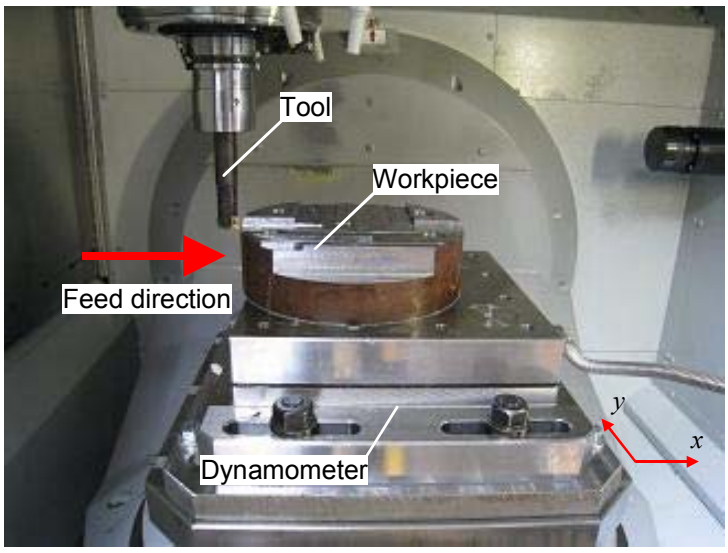

Figure 8 Experimental setup for milling test

Table 5 Cutting conditions in chatter test

Cutting conditions	Feed rate mm/tooth	0.10
	Axial depth of cut mm	0.45-2.00
	Immersion	Slot Milling
	Spindle speed min^{-1}	1500-3500
Tool	Diameter mm	20
	Insert type	R390-11 T3 02E-PM
	Number of flutes	2
Workpiece	Material	AISI 1045
Modal Parameters in – x direction	k_x N/μm	18
	ζ_x	0.039
	ω_{nx} Hz	1744
Modal Parameters in – y direction	k_y N/μm	17
	ζ_y	0.089
	ω_{ny} Hz	1894

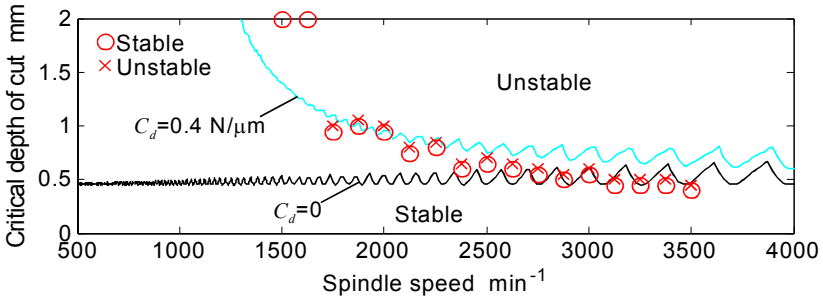

Figure 9 Comparison of predicted and measured chatter stability in milling (See Table 5 for cutting conditions.)

5. Conclusions

Process damping in dynamic metal cutting has been difficult to model, although it plays an important role in damping chatter in low-speed turning and milling of steel and thermally-resistant aerospace alloys. This paper presents in process identification of process damping coefficient from simple turning tests. Process damping is identified from the characteristic equation of the turning process when it is critically stable during cutting tests. It is shown that once tool wear reaches a level that covers the vibration wave left on the surface, process damping becomes fully effective and additional tool wear does not significantly change the damping during the process.

The process damping coefficient identified from turning tests has been adopted in assessing the stability of milling operations at low speeds. Despite the differences in insert geometry, vibration frequency, and the kinematics of cutting processes, the process damping coefficient identified from turning tests could be effectively used in predicting stability charts in milling. It can be concluded that the process damping is highly dependent upon the contact mechanics between the wavy surface finish of the workpiece material and the clearance face of the cutting tool.

References

(1) Tlusty, G., Manufacturing Process and Equipment, Prentice Hall (1999), pp. 559-579.

(2) Altintas, Y. and Weck, M., Chatter Stability in Metal Cutting and Grinding, *Annals of the CIRP*, Vol. 53, No. 2 (2004), pp. 619-642.

(3) Sisson, T.R. and Kegg, R.L., An Explanation of Low-speed Chatter Effects, *ASME Journal of Engineering for Industry*, Vol. 91 (1969), pp. 951-958.
(4) Hoshi, T., Cutting Dynamics Associated with Vibration Normal to Cut Surface, *Annals of the CIRP*, Vol. 21, No. 1 (1972), pp. 101-102.
(5) Tlusty, J., Analysis of the state of research in cutting dynamics, *Annals of the CIRP*, Vol. 27, No. 2 (1978), pp. 583-589.
(6) Montgomery, D. and Altintas, Y., Mechanism of Cutting Force and Surface Generation in Dynamic Milling, *ASME Journal of Engineering for industry*, Vol. 113 (1991), pp. 160-168.
(7) Lee, B. Y., Tarng, Y. S. and Ma, S. C., Modeling of the Process Damping Force in Chatter Vibration, *International Journal of Machine Tools Manufacture*, Vol. 35, No. 7 (1995), pp. 951-962.
(8) Clancy, B. E. and Shin, Y. C., A Comprehensive Chatter Prediction Model for Face Turning Operation Including the Tool Wear Effect, *International Journal of Machine Tools and Manufacture*, Vol. 42 No. 9 (2002), pp. 1035-1044.
(9) Altintas, Y., Eynian, M., and Onozuka, H., Identification of Dynamic Cutting Force Coefficients and Chatter Stability with Process Damping, *CIRP Annals Manufacturing Technology*, Vol. 57, No. 1 (2008), pp. 371-374.
(10) Suzuki, N., Kurata, Y., Hino, R., and Shamoto, E., Identification of transfer function of mechanical structure by inverse analysis of generative chatter vibration in end milling, *Proceedings of 3rd International Conference on High Performance Cutting*, Dublin (2008), pp. 455-463, (CD-ROM).
(11) Colwell, L. V. and Arbor, A., Predicting the Angle of Chip Flow for Single-Point Cutting Tools, *Transactions of the ASME* (1954), pp. 199-204.
(12) Altintas, Y. and Budak, E., Analytical Prediction of Stability Lobes in Milling, *Annals of the CIRP*, Vol. 44, No. 1 (1995), pp. 357-362.